Monterey Bay Aquarium
Research Institute

Estimating Primary Productivity from Diel Measurements of Oxygen and pH from Autonomous Gliders

Stephen Huie, California Polytechnic State University, San Luis Obispo

Mentors: Yui Takeshita

Summer 2021

Keywords: primary productivity, autonomous gliders, diel cycles, pH

ABSTRACT

Gross primary productivity (GPP) refers to the amount of organic carbon fixed by phytoplankton in the ocean. GPP is a critical parameter because of its strong influence on the biological carbon pump, food web, and fisheries industry. Historically, ^{14}C isotope bottle incubations have been the standard methodology for measuring GPP but have inherent biases ignoring in situ conditions or the “bottle effect”. Previous studies have found that diel cycles of O_2 from gliders can reliably estimate GPP in the open ocean but are required to assume metabolic quotients to convert O_2 into carbon which may lead to uncertainties. We were interested in the possibility of using autonomous gliders equipped with pH sensors to measure diel cycles of dissolved inorganic carbon (DIC) directly with algorithm-derived total alkalinity (TA). Compared to previous GPP glider studies done in the open ocean, we focused closer to shore (within 300 km of Monterey Bay, CA) and looked at a glider survey from February 2021. Using the method from Barone et al., 2019, we found the average GPP from O_2 and DIC diel cycles to be 2.092±0.148 and 1.362±0.213 mmol C m^{-3} d^{-1} respectively. We found the average ratio of oxygen to carbon to be 1.663±0.244 mol O_2 mol C^{-1} during photosynthesis (PQ) and 1.456±0.246

during respiration (RQ). Our estimates for GPP did not align with previous study estimates which may be due to not accounting for depth, air-sea gas exchange, diapycnal mixing, or differences in location. We found that salinity normalization introduced the largest uncertainties for GPP from diel DIC cycles compared to other methods used to calculate the diel cycle of DIC.

INTRODUCTION

Primary productivity (PP) is an important parameter because it is the initial measurement of how much energy will be available in the ocean food chain, providing energy for fish populations and supporting fisheries (Pauly & Christensen, 1995). In addition to PP's strong influence on the biological carbon pump, it helps regulate the air-sea gas exchange of CO2 and produce oxygen, both driven by photosynthesis and respiration. Despite the importance of PP to the ocean carbon cycle and ecosystems, the ability to accurately measure and standardize PP rates is limited by the methodology behind it. For most of oceanography's history, the most utilized method to measure PP is to use ^{14}C bottle incubations (Nielsen, 1952). Despite its long history of usage, many of the flaws of the ^{14}C incubation method have been acknowledged (Peterson, 1980). These include the 'bottle effect', the exclusion of grazing, and the assumption of in-situ conditions of light and temperature (Bender et al., 1987).

With the desire to measure ocean PP in situ to minimize known biases in the ^{14}C-PP method, other scientists have developed methods to characterize metabolic rates that do not rely on incubations. For example, previous studies used autonomous gliders to investigate daily changes in O_2 in oligotrophic open ocean regions to find estimates of PP in situ above the mixed layer (Nicholson et al., 2015; Barone et al., 2019). These daily changes in parameters such as O_2 are driven by biological processes, for example, increasing O_2 during the day from photosynthesis and decreasing at night due to respiration. These consistent up and down patterns occur over the course of 24 hours and are called diel cycles. Nicholson et al. 2015 and Barone et al. 2019 fitted a model based on a photo irradiance curve to O_2 diel cycles to estimate gross primary productivity (GPP) and community respiration (CR) above the mixed layer. In addition to GPP and

CR derived from autonomous glider O_2 diel cycles, GPP estimates have been calculated from cruise sampling in the open ocean looking at diel cycles of O_2 and particulate organic carbon (POC).In this approach, they calculated GPP and CR by interpreting the daily minima and maxima as the total production per day, rather than fitting a model to the data(White et al., 2017; Henderikx et al., 2020). In addition to finding GPP and CR estimates, Henderikx et al., 2020 was interested in finding the photosynthetic quotient (PQ) and respiration quotient (RQ) which are the ratios of oxygen to carbon produced or consumed during photosynthesis and respiration respectively. They found an average PQ of ~1.4 ± 0.2 and RQ of ~1.0 ± 0.2 mol O_2 mol C with no significant difference between subtropical and subpolar regionals for both (Henderikx et al., 2020).

This provided evidence that diel cycles of O_2 and POC can be used to estimate GPP and CR primarily in open oceans; however, the open ocean differs from the coastal environment. The oligotrophic open ocean is lower in nutrients and has less biological activity. This project investigated the waters off the coast of Monterey, CA, a part of the California Current System, and is a prime location for wind-driven upwelling and high biological activity. (Carr & Kearns, 2003). Measuring PP in these environments is important to learn more about the movement of energy through the food chain and quantifying carbon export for predicting fisheries yields (Friedland et al., 2012). However, the highly productive environment comes with additional challenges. Variability from physical and processes in the coastal environment such as upwelling may add more noise making it more difficult to isolate diel cycles relative to the open ocean.

Despite being successful in measuring GPP and CR from O_2 and POC diel cycles, there are some concerns from these measurements. Nicholson et al., 2015 and Barone et al., 2019 used O_2 concentration and were required to assume metabolic quotients to convert oxygen to carbon measurements which could lead to uncertainties in GPP in carbon units. White et al., 2017 and Henderikx et al., 2020 used POC as a more direct approach to quantify GPP for carbon; however, POC does not account for all the carbon present such as dissolved organic carbon. Additionally, they did not use gliders to collect carbon-based measurements, which limits their ability to resolve spatiotemporal variability. To measure the overall carbon pool involved in photosynthesis/respiration, we focused on the potential of using autonomous gliders and pH to estimate GPP. Recently, the deep sea durafet pH sensor was integrated onto the Spray underwater glider (Takeshita et al. 2021), providing a novel tool to enable this study. By measuring two of any of the four ‘master’ carbonate parameters, pH, total alkalinity (TA), dissolved inorganic carbon (DIC), or partial pressure of CO2 (pCO2), it is possible to estimate the others based on in-situ conditions. With pH measurements and estimated TA from in-situ parameters, we could calculate GPP from DIC.

To better understand PP, we investigated the accuracy and reliability of using O2 and pH calculated DIC diel cycles collected by autonomous gliders to estimate GPP in the coastal environment. Based on GPP and CR measurements, we asked what are the ratio of oxygen to carbon produced and consumed during photosynthesis and respiration respectively? We are interested in what method is the best way to calculate GPP and CR, how DIC should be calculated from total alkalinity, and what are other processing steps are needed.

MATERIALS AND METHODS

The glider mission was conducted by The Monterey Bay Aquarium Research Institute (MBARI), with a Spray underwater glider from February 2021 to May 2021. The spray glider was equipped with additional sensors including a Deep-Sea DuraFET pH sensor, a SBE63 oxygen sensor, and CTD. To remain in the same water mass, a section of the glider path in the center of an eddy about 300 km from the coast of Monterey, CA was examined (Figure 1).

To determine the most appropriate way to estimate GPP, DIC was calculated using several approaches by altering how TA values were calculated. These variations were using a constant TA value of 2200 μmol/kg and measured pH, nutrient concentrations, and TA estimated using CANYON-B (Bittig et al., 2018). An additional TA value was a constant daily average which assumed TA did not change significantly over the course of a day and was determined by a linear relationship between TA from CANYON-B and salinity. Using recorded in situ pH, a TA option, and other CANYON-B output, the Matlab edition of CO2SYS was used to estimate DIC with dissociation constants from Mehrbach et al., 1973 refit by Dickson and Millero, 1987 (Lewis and Wallace, 1998; Van Heieven et al., 2011).

Figure 1: Glider path taken from February 2021 to May 2021. Each pin represents a data point. The blue pin represents MBARI. Green points represent the beginning and endpoints of the glider section analyzed. The red circle highlights the area of the section chosen.

PRODUCING DIEL CYCLES

To isolate biological processes, mainly, photosynthesis and respiration, for O_2 and DIC diel cycles, several steps were taken to remove variability from physical processes. Temperature variability was accounted for by calculating the anomaly between O_2 concentration and O_2 saturation. Because oxygen equilibrates with the atmosphere quickly and O_2 concentration will vary depending on the temperature, by adjusting for O_2 saturation, variability in O_2 concentration due to gas exchange was reduced. To remain consistent, similar calculations were done for DIC anomalies by comparing each DIC variation to reference DIC saturation values. Reference DIC saturation values were calculated using the same Matlab CO2SYS configurations but used the appropriate TA variation and pCO_2 of 416 μatm based on the Keeling curve (Keeling & Keeling, 2017). In addition to saturation adjustments, a reference salinity value of 32.625 PSU was used to normalize DIC values. To reduce the amount of noise, O_2 and DIC data were partitioned into 5 m depth bins from the surface to 30 m. Upon binning data, depth profiles for each time were visually inspected and removed if they deviated from surrounding profiles. For each depth bin, the anomaly data for O_2 and DIC was calculated by subtracting the daily mean or detrending to account for low-frequency variability caused by physical processes. After isolating the influence of biological processes, data was parsed into hourly bins to create a diel cycle for each day at each depth bin. Diel cycles were averaged to create a composite plot representative of the top 30 m of an average day for oxygen and each DIC permutation.

GPP, CR, and initial oxygen concentration (C_0) were estimated using a model presented in Nicholson et al., 2015, and updated by Barone et al., 2019. The model produces three different fits (linear, sinusoidal, and PvE), but only results calculated from the sinusoidal fit are presented here as suggested by Barone et al., 2019. For O_2 diel cycles, the same code as Barone et al., 2019 was used, but for DIC, the code was modified for carbon measurements since it would be inverted of O_2. Because the fit model used predicted irradiance of a specific location and time, date, time, and location, were important input parameters. Time for all diel cycles was set in hour intervals starting at a half-hour past midnight to represent the whole day evenly. The day, latitude, and longitude were determined by the median day based on the number of days incorporated into the diel cycle. Overall, similar dates and coordinates did not have a noticeable impact on estimates, but the timing of each point strongly influenced the fit model. Based on estimated GPP and CR outputs from the composite plots, metabolic quotients were calculated by finding the ratio of GPP and CR from oxygen and carbon, described by Henderikx et al., 2020.

$$\text{Photosynthetic Quotient (PQ)} = \text{GPP}_{\text{O2}}/\text{GPP}_{\text{DIC}}$$

$$\text{Respiration Quotient (RQ)} = \text{CR}_{\text{O2}}/\text{CR}_{\text{DIC}}$$

RESULTS

It is important to note that diel cycles were innately present in the data without modification. In a time series plot (Figure 2), diel cycles for O_2, pH, and DIC can be clearly seen. While there was additional frequency variability, there was a consistent up and down cycle for each of the three parameters. Between the O_2 and pH and DIC, they followed the same overall trend, but DIC was inverted. This was expected as O2 increased due to photosynthesis byproduct during the day, DIC decreased as CO_2 was consumed, and vice versa, as O_2 decreased at night from net respiration, DIC increased. pH followed the same trend as O_2.

Figure 2: Time series of O_2 (a), pH (b), and DIC (c). Red open circles in (a) and (b) represent outlier data that has been removed prior to calculations. The various colored lines in (c) correspond to a different TA calculation to estimate DIC.

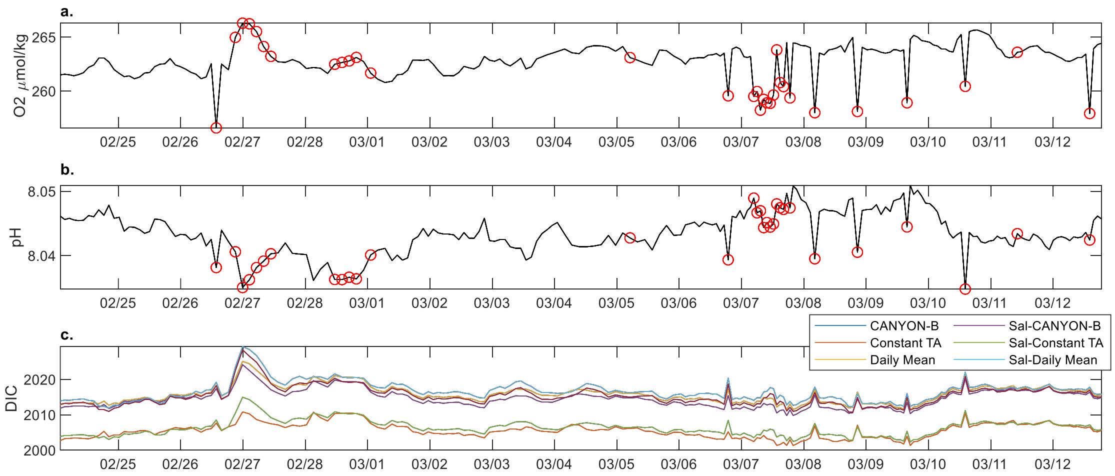

Estimating rates for GPP and CR from O_2 were divided based on diel cycles subtracting the daily mean or detrending. In Figure 3, there were clear diel cycles for both anomaly methods. Although there was some variation in patterns and magnitudes, they both followed the same general trend that was expected from an O_2 diel cycle (decreased at night and increasing during the day). The daily mean adjusted diel cycle had more depth-dependent variation before the increase in O_2 while the remaining part of the day and the whole day of the detrended diel cycle remains consistent between all depths. Because there was minimal variability between different depths and to reduce noise, depths were averaged to get one diel cycle representative of the top 30 m. Figure 4 shows the composite plot of the top 30 m and highlights differences between subtracting the daily mean and detrending. Overall, both diel cycles followed the same general trend with the daily mean adjusted diel cycle having a larger magnitude peak and trough compared to the detrended diel cycle. Composite diel cycles were used with the fit model from Barone et al., 2019 to produce estimates for GPP and CR (Table 1).

Figure 3: Shows depth binned diel cycles for ΔO_2 between O_2 concentration and daily mean O_2 saturation over a 24 hr period. (a) is for daily mean adjusted diel cycles, and (b) is detrended diel cycles. The different colored lines identify the depth of the diel cycle ranging from 1m to 30 m. The dotted line is to help visualize ΔO_2 above and below 0.

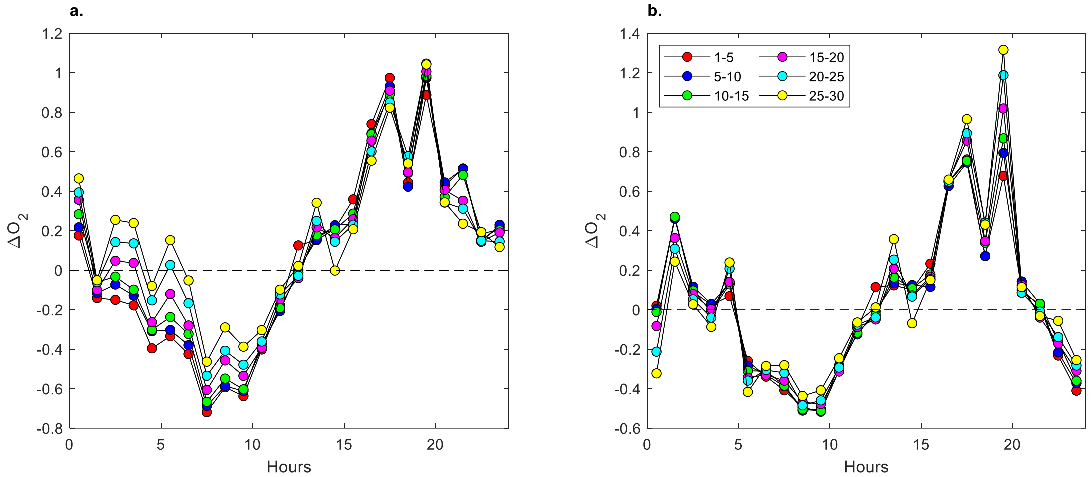

Figure 4: (a) Shows average composite diel cycles for ΔO_2 between O_2 concentration and O_2 saturation over a 24 hr period. The different lines identify the ΔO_2 calculation: daily mean adjusted (red), detrended (blue). The dotted line is to help visualize ΔO_2 above and below 0.

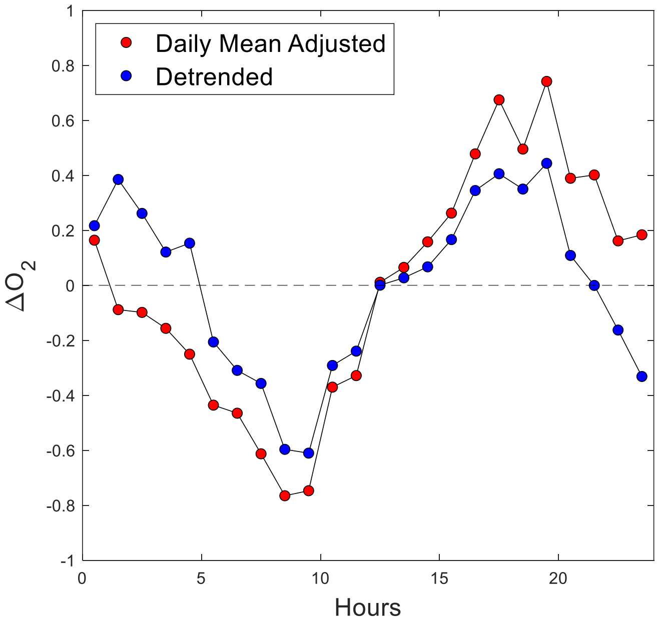

Like O_2, GPP and CR estimates were derived from the different DIC variation diel cycles and were separated based on subtracting the daily mean and detrending and if salinity was normalized. To remain consistent with O_2 (Figure 5), the fit model was used with the average composite of the top 30 m for DIC diel cycles. While Figure 5 only showed daily mean adjusted diel cycles, both daily mean adjusted and detrended diel cycles had minimal variation between the different TA-derived DIC diel cycles. Since the three TA variations to calculate DIC produced similar results (Figure 5), Figure 6 used CANYON-B derived TA as a representative for other DIC calculations. Comparing daily mean adjusted and detrended DIC, the first six hours of the daily mean adjusted and detrended diel cycles did not line up; however, after reaching the first peak, both diel cycles followed each other relatively close (Figure 6a). Between salinity normalized and non-normalized DIC, salinity normalized appeared to have a larger anomalies, particularly during the day as DIC decreases (Figure 6b). This corresponded with GPP and CR estimates (Table 2) that salinity normalized DIC estimates were higher relative to non-normalized. These together suggest that daily mean adjusted and detrended caused less variability compared to whether DIC was salinity normalized.

Figure 5: Shows average composite diel cycles for ΔDIC between DIC and daily mean DIC reference saturation over a 24 hr period. The different lines identify the different TA variations used to calculated DIC: TA from CANYON-B (red), constant TA of 2200 (blue), and daily mean TA (green). The dotted line is to help visualize ΔDIC above and below 0.

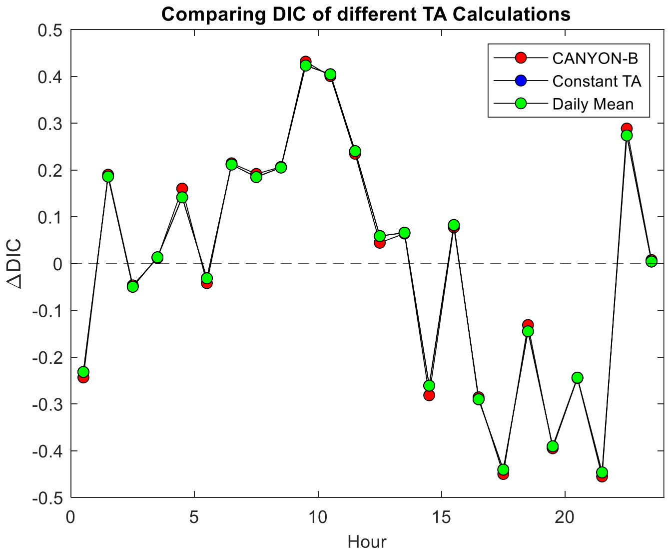

Figure 6: (a) Shows average composite diel cycles for ΔDIC between CANYON-B derived TA calculated DIC and DIC reference saturation over a 24 hr period. The different lines identify the different anomaly calculation methods: daily mean adjusted (red) or detrended (blue). (b) The different lines identify if the DIC has been salinity normalized (cyan) or not (magenta). The dotted line is to help visualize ΔDIC above and below 0.

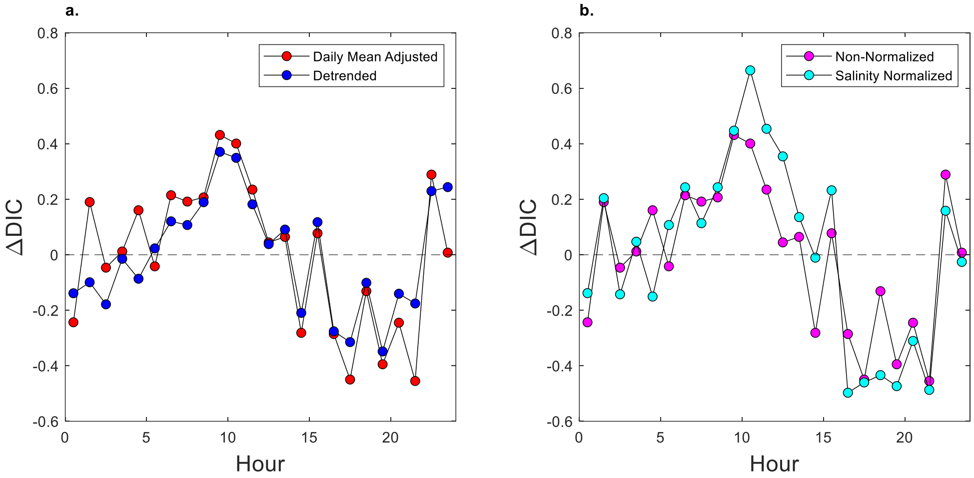

Because there were several different DIC and anomaly variations, GPP and CR estimates for all combinations were organized to assess differences between the permutations to determine the best way to estimate GPP and quotients. The three TA variations to calculate DIC were averaged based on salinity normalization and anomaly method for a total of four values with their own GPP, CR, PQ, and RQ. For both daily mean adjusted and detrended rates, salinity normalized had larger GPP and CR values compared to non-normalized, and daily mean adjusted had a larger GPP and lower CR values estimates compared to detrended. When comparing the overall averages of GPP and CR, we found that our CR was greater than GPP, suggesting net respiration. There did not appear to be any patterns between the different permutations and PQ and RQ values; however, the PQ was always greater than the corresponding RQ (Table 2).

Table 1: Average and standard deviations from O2 variations based on daily mean adjusted or detrended.

	Daily	**Detrended**	**Average**
GPP mmol O m^{-3} d^{-1}	2.2	1.99	2.092±0.148
CR mmol O m^{-3} d^{-1}	2.19	2.74	2.467±0.387
$\mathbf{R^2}$	0.93	0.85	

Table 2: Average and standard deviations from each DIC variation based on whether it was salinity normalized and daily mean adjusted or detrended.

	Daily		**Detrend**		**Average Rates**
	Non-Normalized	**Normalized**	**Non-Normalized**	**Normalized**	
GPP mmol C m^{-3} d^{-1}	1.23±0.004	1.605±0.003	1.141±0.005	1.47±0.004	1.362±0.213
CR mmol C m^{-3} d^{-1}	1.414±0.006	1.848±0.005	1.567±0.005	2.05±0.004	1.72±0.284
PQ mol O_2 mol C^{-1}	1.786±0.006	1.369±0.003	1.573±0.139	1.924±0.008	1.663±0.244
RQ mol O_2 mol C^{-1}	1.551±0.006	1.187±0.003	1.749±0.006	1.337±0.003	1.456±0.246

DISCUSSION

Comparing GPP and CR values from O_2 and DIC diel cycles to previously recorded values, our estimates did not fall within previously recorded ranges possibly due to location and seasonality. Our average O_2 derived GPP of 2.09 ± 0.148 and CR of 2.47 ± 0.387 mmol O2 m^{-3} d^{-1} were greater than subtropical open ocean expected average GOP 1.33 ± 0.04 and CR 1.25 ± 0.33 mmol O_2 m^{-3} d^{-1}; however, they were lower than the subpolar Alaskan coast expected average GOP 4.43 ± 0.74 and CR 3.61 ± 0.91 mmol O_2 m^{-3} d^{-1} (Henderikx et al., 2020). For both subtropical and subpolar estimates, Henderikx et al, found that GPP was greater than CR suggesting net production, but our results were the opposite. Similarly, all our average DIC-derived GPP 1.362 ± 0.213 and CR 1.72 ± 0.284 were greater than subtropical open ocean expected average GCP 1.09 ± 0.29 and CR 1.07 ± 0.2 mmol C m^{-3} d^{-1}; however, they were lower than the subpolar Alaskan coast expected average GCP 3.18 ± 0.8 and CR 3.94 ± 1.55 mmol O_2 m^{-3} d^{-1} (Henderikx et al., 2020). Unlike O_2, while all Henderikx et al., GPP estimates were greater than CR, for DIC-derived subpolar estimates, CR was greater than GPP, like ours. The differences in estimates can be due to a couple of possible reasons, (1) Henderikx et al. used the linear diel fit model which tended to differ from the sinusoidal. (2) The location they collected data from is not a fair comparison to our location. While the subtropic region is at a similar latitude, which is important since the estimates are lightdependent, it was not unexpected that we would find a greater GPP in the coastal region likely driven by higher nutrient concentrations near the coast. On the other hand, the subpolar region is a coastal environment, but the latitude and light differences may affect productivity and results. (3) Another factor is seasonality. Our GPP values were lower than subpolar despite both being productive coastal regions; however, our data was collected during February, an expected low productive season while Henderikx et al., data was collected during September, a more productive season.

With several GPP and CR estimates based on different DIC calculations we calculated several PQ and RQ estimates, but we founded that our RQ averages were closer to expected ranges compared to PQ. For PQ, there was an expected range between 1.1 and 1.4 mol O_2 mol C^{-1} based on NH_4 and NO_3 uptake (Laws, 1991). Our average PQ 1.663±0.244 mol O_2 mol C^{-1} was greater than the expected range, and our only value within the range was the daily mean adjusted, salinity normalized PQ of 1.369 ± 0.003 mol O_2 mol C^{-1}. While our average PQ was not within the expected range, based on the standard deviation, it remained at the high end of the range. For RQ, results were more agreeable with expected values. The average phytoplankton composition was expected to have an average RQ of 1.45 mol O_2 mol C^{-1} ranging from 1.0 to 1.55 mol O_2 mol C^{-1} depending on different metabolic sources of energy (1.0 from carbohydrates, 1.45 from lipids, 1.55 from proteins) (Hedges et al., 2002; Laws, 1991). All our RQ estimates fell within this range except for the detrended, non-normalized RQ of 1.749±0.006 mol O_2 mol C^{-1}. Additionally, our average RQ estimate was 1.456±0.246 mol O_2 mol C^{-1} and was very similar to the expected average RQ and implied the respiring of lipids; however, individual values ranged closer to respiring from carbohydrates and others from respiring proteins. Since our average PQ was greater than our average RQ, this suggests that more oxygen was produced than consumed. Our average PQ and RQ were within or close to the expected ranges which suggest that the relationship to GPP and CR was correct, but the rate estimate themselves were off by the same amount from expected values.

Based on differences between averages and standard deviations of the GPP and CR rates from O_2 and the different DIC permutations, it suggests that salinity normalization had a strong influence on GPP and CR compared to different anomaly calculations and different TA values. For O_2, there was about a 10.0% GPP and 22.3%

CR difference between daily mean adjusted and detrended. For DIC, between daily mean adjusted and detrended rates (Table 2), there was about a 7 - 10% difference in GPP and CR. Since differences between daily mean adjusted and detrended estimates were small, we conclude that the method to calculate the diel anomaly has minimal influence on GPP and CR rates. However, when comparing the influence of salinity normalization, there was about a 25 - 26% difference between salinity normalized and non-normalized GPP and CR, indicating that salinity normalization had a greater influence on GPP and CR rates. Additionally, low standard deviations for GPP and CR averages (Table 2) confirms from Figure 5 that there was minimal variation between predicted DIC when calculating with different TA values. When determining the best method to estimate GPP, this suggests that different values for TA and anomaly calculations for DIC account for less variation than if DIC has been salinity normalized or not.

FUTURE STEPS

To better assess these results, there are several possible sources of variation left to be account for, and the analysis should be repeated, but in different conditions to test the validity of the model. While diel cycles were averaged to produce one composite diel cycle of the top 30 m for consistency, this may be ignoring depth-dependent variation found in O_2 and DIC. We would anticipate a depth-dependent decrease in productivity due to decreased light availability at depth. In addition to depth variation, we did not account for air-sea gas exchange and diapycnal mixing. While Barone et al., 2019 found that these have negligible influence in the open ocean this may prove otherwise in the coastal region, as O_2 was supersaturated by 5-6% at times. Different values of TA were found to have minimal influence when calculating DIC, there may be other TA values or processing steps like salinity normalization to more accurately represent DIC. Then to confirm our results, future studies should repeat this analysis in similar locations and different seasons, as well as directly measure productivity rates alongside glider observations. We can check to see how our results compare in similar locations or how the seasonality of temperature or nutrients levels may affect GPP and CR. Because O2 estimates are reliant on temperature to produce saturation anomalies, temperature changes may drastically change estimates despite having similar PP values. Regardless of comparing results, additional deployments in different locations can help characterize PP in the ocean at a lower cost to cruise ships and bottle measurements.

CONCLUSIONS/RECOMMENDATIONS

Based on our average results, it seems that we can produce GPP and CR estimates from O2 and DIC diel cycles from autonomous gliders. Despite having uncertain values relative to expected ranges, our GPP and CR estimates were not obscure and produced PQ and RQ estimates within or close to expected ranges. We were successful in producing preliminary estimates since the variation from physical processes has not been accounted for, and it is uncertain if the Monterey region is a valid comparison to previous studies' results. While we did not find the best method when estimating GPP and CR, we did find that different TA values had little impact when calculating DIC. There is some variation between anomaly calculations of the daily mean and detrending, but it is minimal in comparison to the variation caused by salinity normalization which will be an important factor in future attempts.

ACKNOWLEDGEMENTS

Thank you to the CSUMB REU, NSF, and MBARI for providing funding and this opportunity. Special thanks to my mentor Yui Takeshita for his guidance and help, the REU directors: Corey Garza, Laura Good, and Juliana Cornett; and the MBARI intern directors: George, Megan, and Lyndsey for their support.

References:

Barone, B., Nicholson, D., Ferrón, S., Firing, E., & Karl, D. (2019). The estimation of gross oxygen production and community respiration from autonomous time-series measurements in the oligotrophic ocean. Limnology and Oceanography: Methods, 17(12), 650-664.

Bender, M., Grande, K., Johnson, K., Marra, J., Williams, P. J. L., Sieburth, J., ... & Heinemann, K. (1987). A comparison of four methods for determining planktonic community production 1. Limnology and Oceanography, 32(5), 1085-1098.

Bittig, H. C., Steinhoff, T., Claustre, H., Fiedler, B., Williams, N. L., Sauzède, R., ... & Gattuso, J. P. (2018). An alternative to static climatologies: Robust estimation of open ocean CO2 variables and nutrient concentrations from T, S, and O2 data using Bayesian neural networks. *Frontiers in Marine Science*, *5*, 328.

Carr, M. E., & Kearns, E. J. (2003). Production regimes in four Eastern Boundary Current systems. Deep Sea Research Part II: Topical Studies in Oceanography, 50(22-26), 3199-3221.

Dickson, A. G., & Millero, F. J. (1987). A comparison of the equilibrium constants for the dissociation of carbonic acid in seawater media. *Deep Sea Research Part A. Oceanographic Research Papers*, *34*(10), 1733-1743.

Friedland, K. D., Stock, C., Drinkwater, K. F., Link, J. S., Leaf, R. T., Shank, B. V., ... & Fogarty, M. J. (2012). Pathways between primary production and fisheries yields of large marine ecosystems. *PloS one*, *7*(1), e28945.

Hedges, J. I., Baldock, J. A., Gélinas, Y., Lee, C., Peterson, M. L., & Wakeham, S. G. (2002). The biochemical and elemental compositions of marine plankton: A NMR perspective. *Marine Chemistry*, *78*(1), 47-63.

Henderikx Freitas, F., White, A. E., & Quay, P. D. (2020). Diel Measurements of Oxygen-and Carbon-Based Ocean Metabolism Across a Trophic Gradient in the North Pacific. *Global Biogeochemical Cycles*, *34*(11), e2019GB006518.

Keeling, R. F., & Keeling, C. D. (2017). Atmospheric monthly in situ CO2 data-mauna loa observatory, Hawaii. *Scripps CO2 program data*. Accessed on August 6, 2021.

Mehrbach, C., Culberson, C. H., Hawley, J. E., & Pytkowicx, R. M. (1973). Measurement of the apparent dissociation constants of carbonic acid in seawater at atmospheric pressure 1. *Limnology and oceanography*, *18*(6), 897-907.

Laws, E. A. (1991). Photosynthetic quotients, new production and net community production in the open ocean. *Deep Sea Research Part A. Oceanographic Research Papers*, *38*(1), 143-167.

Lewis, E. R., & Wallace, D. W. R. (1998). *Program developed for CO2 system calculations* (No. cdiac: CDIAC-105). Environmental System Science Data Infrastructure for a Virtual Ecosystem.

Nicholson, D. P., Wilson, S. T., Doney, S. C., & Karl, D. M. (2015). Quantifying subtropical North Pacific gyre mixed layer primary productivity from Seaglider observations of diel oxygen cycles. *Geophysical Research Letters*, *42*(10), 4032-4039.

Pauly, D., & Christensen, V. (1995). Primary production required to sustain global fisheries. *Nature*, *374*(6519), 255-257.

Peterson, B. J. (1980). Aquatic primary productivity and the 14C-CO2 method: a history of the productivity problem. *Annual Review of Ecology and Systematics*, *11*(1), 359-385.

White, A. E., Barone, B., Letelier, R. M., & Karl, D. M. (2017). Productivity diagnosed from the diel cycle of particulate carbon in the North Pacific Subtropical Gyre. *Geophysical Research Letters*, *44*(8), 3752-3760.

van Heuven, S., Pierrot, D., Rae, J. W. B., Lewis, E., & Wallace, D. W. R. (2011). MATLAB Program Developed for CO2 System Calculations. Oak Ridge, Tennessee: ORNL/CDIAC-105b. Carbon Dioxide Information Analysis Center, Oak Ridge National Laboratory, US Department of Energy.

Takeshita, Y., Jones, B. D., Johnson, K. S., Chavez, F. P., Rudnick, D. L., Blum, M., ... & Warren, J. K. (2021). Accurate pH and O2 measurements from spray underwater gliders. Journal of Atmospheric and Oceanic Technology, 38(2), 181-195.